SPE-190321-MS

Beneficial Relative Permeabilities for Polymer Flooding

R. S. Seright, New Mexico Tech; Dongmei Wang, University of North Dakota; Nolan Lerner, Anh Nguyen, Jason Sabid, and Ron Tochor, Cona Resources Ltd

This paper was prepared for presentation at the SPE Improved Oil Recovery Conference held in Tulsa, Oklahoma, USA, 14-18 April 2018.

Abstract

This paper examines oil displacement as a function of polymer solution viscosity during laboratory studies in support of a polymer flood in the Cactus Lake reservoir in Canada. When displacing 1610-cp crude oil from field cores (at 27°C and 1 ft/d), oil recovery efficiency increased with polymer solution viscosity up to 25 cp (7.3 s^{-1}). No significant benefit was noted from injecting polymer solutions more viscous than 25 cp. Much of the paper explores why this result occurred. That is, was it due to the core, the oil, the saturation history, the relative permeability characteristics, emulsification, or simply the nature of the test? Floods in field cores examined relative permeability for different saturation histories—including native state, cleaned/water-saturated first, and cleaned/oil-saturated first. In addition to the field cores and crude oil, studies were performed using hydrophobic (oil-wet) polyethylene cores and refined oils with viscosities ranging from 2.9 to 1000 cp. In nine field cores, relative permeability to water (k_{rw}) remained low—less than 0.03 for water saturations up to 0.42. Relative permeability to oil (k_{ro}) remained reasonably high (greater than 0.05) for most of this range. At a given water saturation, k_{rw} values for 1000-cp crude oil were about ten times lower than for 1000-cp refined oil. These observations help explain why only 25- cp polymer solutions were effective in recovering the viscous crude oil. In contrast to results found for the Daqing polymer flood, no evidence was found that high-molecular-weight (Mw) HPAM solutions mobilized trapped residual oil in our application. The results are discussed in light of ideas expressed in recent publications. The relevance of the results to field applications is also examined. Although 25-cp polymer solutions were effective in displacing oil during our core floods, the choice of polymer viscosity for a field application must consider reservoir heterogeneity and the risk of channeling/viscous fingering in a reservoir.

Introduction

The concentration and viscosity of polymer used in a polymer flood is of critical importance. On the one hand, use of too much polymer can jeopardize the economics of a flood. On the other hand, use of insufficient polymer can promote channeling/viscous fingering and the problems associated with early polymer breakthrough. In several field polymer floods in Canada, 15-30-cp polymer solutions were injected to displace 1000-3000-cp oil (Wassmuth et al. 2009, Liu et al. 2012, Delamaide et al. 2014, Saboorian-Jooybari et al. 2015). Waterflooding has also been applied in a number of cases (Beliveau 2009, Kumar et

al. 2008). Controversy exists about whether improved results might be seen if greater polymer viscosities were injected. A number of arguments have been offered on both sides of this discussion (Seright 2017). Arguments that have been made in favor of using low polymer viscosities include: (1) the relative permeability to water may be surprisingly low, (2) mobility ratio at the oil-water shock front is much lower than the endpoint mobility ratio, (3) economics favor using low polymer viscosities, (4) high polymer resistance factors and residual resistance factors reduce the need for high polymer viscosities and volumes, (5) high-viscosity polymer solutions unreasonably impair injectivity, and (6) polymers can emulsify oil in situ—leading to higher than expected resistance factors (Vittoratos and Kovscek 2017).

Seright (2017) argued that Reasons 2 through 5 above are not generally valid. Concerning Reason 2, the mobility ratio at the shock front was shown not to correlate well with displacement efficiency. Rebutting Reason 3, up to a definable point, higher polymer concentrations are economically favored because (a) solution viscosity increases roughly with the square of polymer concentration, (b) the value of the oil produced relative to the cost of polymer injected is fairly insensitive to polymer concentration, (c) the cost of surface facilities for producing high polymer concentrations is not greatly more than for producing low polymer concentrations, and (d) efficiently displacing oil with a moderate-to-high polymer viscosity delays polymer breakthrough and the accompanying problems. Concerning Reason 4 above, in moderate-to-high-permeability rock, resistance factors (effective polymer viscosity in porous media) that are more than twice the viscosity or residual resistance factors (permeability reduction values) greater than two are usually laboratory artifacts that will not materialize deep in a reservoir (Seright et al. 2011). Regarding Reason 5 above, polymers are often injected above the formation parting pressure, so injectivity need not be a limitation, so long as fractures don't extend too far (Seright et al 2009, Seright 2017). Reasons 1 and 6 above will be discussed further in this paper.

Wang et al. (2000, 2001a, 2001b, 2010, 2011) advocated injecting very viscous high-molecular-weight polymer solutions to reduce the residual (capillary-trapped) oil saturation below that expected from prolonged waterflooding. A number of authors performed laboratory investigations of this phenomenon—often using fluid velocities that were significantly higher than found in the bulk of most reservoirs (Clark et al. 2015, Koh et al. 2017, Reichenbach-Klinke et al. 2016, Urbissionova et al. 2010, Vermolen et al. 2014). A study by Koh et al. (2017) indicated that at low velocities, the endpoint residual oil satuation was the same for waterflooding and polymer flooding. Recently, Erincik et al. (2017) reported experiments (performed at relatively high velocities) where unusually low residual oil saturations were attained by injecting high-salinity polymer solutions after low-salinity polymer solutions.

This paper examines oil displacement as a function of polymer solution viscosity during laboratory studies in support of a polymer flood in the Cactus Lake reservoir in Canada. A key result is that 25-cp polymer solutions appeared optimum for displacement of 1610-cp crude oil during core floods. Much of the paper explores why this result occurred. That is, was it due to the core, the oil, the saturation history, the relative permeability characteristics, emulsification, or simply the nature of the test? The results are discussed in light of ideas expressed in recent publications. The relevance of the results to field applications is also examined.

Cactus Lake Geological Overview

The Cactus Lake property is located in west-central Saskatchewan in Townships 35 and 36, Ranges 27 and 28 W3M, approximately 40 miles south of Lloydminster, Saskatchewan. Cactus Lake is a heavy oil property, which has been under waterflood since 1988. The largest reservoir in the property produces from the Devonian-Mississippian Bakken Formation and is generally commingled with the Lower Cretaceous Rex Sand. A polymer flood has been under development since 2012, following an extensive vertical drilling program that transitioned the pool from a 40-acre waterflood to a 10-acre polymer flood. At Cactus Lake, heavy oil is produced from the Mississippian aged Bakken and Cretaceous aged Rex Sandstones. The Rex

is in partial-to-full communication with the underlying Bakken via the sub-Cretaceous unconformity and is typically commingled for production with the Bakken.

Bakken

The Lower Mississippian Middle Bakken formation was deposited in a marine shelf environment and later reworked into a series of NE - SW trending sand ridges. The Bakken Formation has three distinct members. The upper and lower members are black organic-rich shales ranging from 3 to 5 m in thickness. The Middle Bakken is typically a very fine to fine grained quartzose sandstone with minor amounts of feldspar, clay and calcite cement. It is commonly unconsolidated, although the base of the sandstone can contain shaley, cemented, non-reservoir sediments. The middle Bakken member reaches a maximum thickness of 30 m. Within the Bakken reservoir, porosities average 30% with permeabilites up to 5.0 Darcies. Water saturations average 37%. Maximum pay thickness is 33 metres while the average pay thickness is 12 m. The area has a relatively gentle SW regional dip that has been modified by numerous Torquay collapse features. Pre-Cretaceous erosion has eroded to the base of the overlying Lodgepole carbonate and commonly into the Bakken sandstone. Oil is trapped both structurally and stratigraphically in the preserved Bakken sandstone.

Rex

The Lower Cretaceous Rex formation was deposited in a deltaic to upper shoreface marine environment. The Rex sandstone directly overlies the sub-Cretaceous unconformity over most of the pool area and is usually separated from the Bakken by a thin (1-4 m) layer of shaley detrital deposits. In some areas, the two sands are in direct communication. The Rex pinches out rapidly to the NW (depositional) and SE (onlap) margins. The Rex sandstone is typically a very fine to fine grained quartzose sandstone which exhibits a coarsening-upwards profile on logs. It is commonly unconsolidated with porosities averaging 30% and permeabilites up to 5.0 Darcies. Water saturations average 30%. Maximum sandstone thickness is 6.5 m while average pay thickness across the pool is 2.7 m. The area has a relatively gentle SW regional dip, and oil is trapped stratigraphically.

Experimental

Fluids

In this work, synthetic Cactus Lake brine contained 17269-ppm NaCl, 114-ppm KCl, 642.4-ppm $CaCl_2$-$2H_2O$, and 919.9-ppm $MgCl_2$-$6H_2O$ (1.9% total dissolved solids, TDS). Two HPAM polymers were used, including SNF Flopaam™ 3630S (copolymer with Mw ~18 million g/mol and 30% degree of hydrolysis) and SNF Flopaam™ 6030S (post-hydrolyzed with Mw ~21 million g/mol and 30% degree of hydrolysis). Polymer solutions were prepared using filtered (through 0.45 μm Millipore filters) brine. The HPAM polymer solutions were prepared by the standard vortex-mixing method. The polymer solutions were not filtered after preparation. At 7.3 s^{-1} shear rate in synthetic Cactus Lake brine at the reservoir temperature of 27°C using 3630S HPAM, 5 cp was achieved with 725-ppm polymer, 25 cp with 1900ppm polymer, 50 cp with 2690-ppm polymer, and 203 cp using 5250 cp. Using 6030S HPAM, 6 cp was achieved with 650-ppm polymer, 25 cp with 1650-ppm polymer, and 52 cp with 2350-ppm polymer. Plots of viscosity versus shear rate for the polymer solutions (at 27°C) are included in Fig. 1. Viscosities were determined using an Anton Paar MCR301 rheometer with CC27-SN29031; d=0 mm measuring system (concentric cylinder).

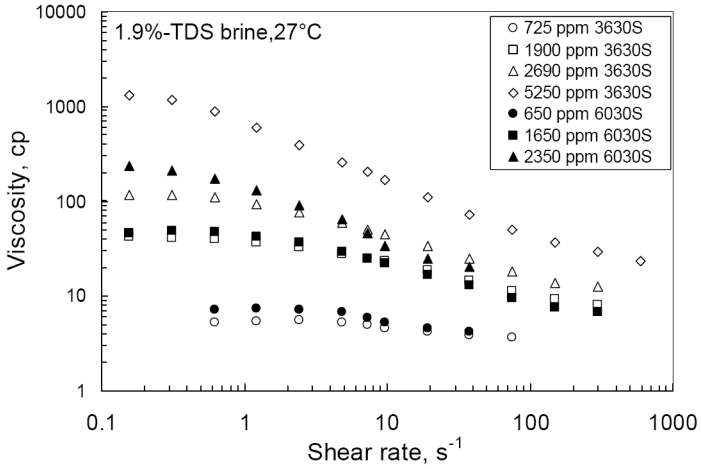

Figure 1—Viscosity versus shear rate for polymer solutions.

At 27°C, Cactus Lake crude oil viscosity ranged from 990 to 1610 cp, depending on the particular sample. For the field core experiments described in Tables 2 and 3 (except Core 1), the oil viscosity was 1610 cp. For the remaining experiments (in Core 1 and the porous polyethylene cores), the crude oil viscosity was 1000 cp. The oil was Newtonian in behavior (viscosity was independent of shear rate). For experiments later in this paper, clear, paraffinic, Newtonian, refined oils were used, with a range of viscosities. Properties of these oils are listed in Table 1. Interfacial tensions were measured against synthetic Cactus Lake brine using the pendant drop method (with a DataPhysics Contact Angle System OCA). All refined oils could pass through a 0.45 μm filter (Millipore) without plugging. Cactus Lake crude oil passed readily through a 5 μm filter without plugging, but not through a 2 μm filter.

Table 1—Properties (at 27°C) of oils used.

Oil	Viscosity, cp	Density, g/cm³	Oil-brine interfacial tension, mN/m
Cactus Lake crude	990-1610	0.960	7.43
Cannon™ S600	1000	0.843	24.3
Equate™ mineral oil	130	0.840	22.9
Cannon™ S20	28	0.855	17.9
Soltrol™ 170	2.9	0.779	13.2

Table 2—Reservoir Core and Flood Properties for HPAM with Mw=18 million g/mol.

Polymer viscosity at 7.3 s^{-1}, 27°C	1	5.2	25.1	50.5	203
Polymer	none	3630	3630	3630	3630
Polymer concentration, ppm	0	725	1900	2690	5250
Core number	1	24	27	26	29
Core length, cm	6.12	6.434	6.11	6.41	6.61
Core diameter, cm	3.81	3.81	3.81	3.81	3.81
Pore volume, cm³	24.5	24.89	23.5	24.5	25.8
Porosity	0.352	0.339	0.338	0.335	0.343
Permeability to oil, md	690*	1142	1100	1635	991
Water breakthrough, PV	0.02	0.059	0.070	0.128	0.107

%OOIP from 1.5 PV water	27.4	29.8	30.5	39.1	43.7
Added %OOIP after 1.5 PV polymer	--	28.7	28.8	28.5	25.7
Added %OOIP after 3 PV polymer	--	39.1	47.1	38.0	33.7
Final %OOIP after polymer	--	72.9	80.1	85.6	82.6
%OOIP for polymer over 1.5 PV water	--	43.1	49.6	46.5	38.9
Added %OOIP after 40 PV of brine	--	3.0	3.3	0.9	1.4
Final S_o	0.301	0.218	0.166	0.135	0.146
Estimated S_{wr}0.22	0.109	~0	~0	0.095	

* Absolute permeability to water was 976 md.

Table 3—Reservoir Core and Flood Properties for HPAM with Mw=21 million g/mol.

Polymer viscosity at 7.3 s^{-1}, 27°C	1	6.1	25.0	52.2
Polymer	none	6030	6030	6030
Polymer concentration, ppm	0	650	1650	2350
Core number	23	20	30	21
Core length, cm	5.736	6.700	6.593	6.477
Core diameter, cm	3.81	3.81	3.81	3.81
Pore volume, cm^3	21.99	24.72	24.50	25.24
Porosity	0.336	0.324	0.326	0.342
Permeability to oil, md	410	206	229	310
Water breakthrough, PV	0.056	0.155	0.071	0.145
%OOIP from 1.5 PV water	15.9	17.2	20.7	18.8
Added %OOIP after 1.5 PV polymer	--	22.5	25.0	23.3
Added %OOIP after 3 PV polymer	--	30.0	31.6	30.2
Final %OOIP after polymer	--	55.9	63.4	56.3
%OOIP for polymer over 1.5 PV water	--	38.7	42.7	37.5
Added %OOIP after 40 PV of brine	--	0.5	1.2	2.0
Final S_o	0.478	0.387	0.314	0.363
Estimated S_{wr}	0.141	0.099	0.113	0.091

Cores and Flooding Procedures

Cactus Lake field cores were 3.81 cm in diameter and 11.40 cm^2 in cross-sectional area. Core length averaged 6.5 cm, porosity averaged 0.33, and pore volume (PV) averaged 24.5 cm^3. Details of the cores and flooding results can be found in Tables 2 and 3. As received (i.e., with the resident oil/water in place), the cores were mounted horizontally in a biaxial Hassler sleeve and applied an overburden pressure of 1500 psi for the duration of the coreflood. A fixed temperature of 27°C was maintained by circulating water from a temperature bath through tubing which was wrapped around the Hassler cell. 100 cm^3 (~4 PV) of crude oil was forced through the core at a flux (Darcy velocity) of 1 ft/d (14.48 cm^3/hr) using a Model 500D ISCO pump. This pump meters fluid in volumes accurate to 0.01 cm^3. For cores flooded with a co-polymerized HPAM with 18×10^6 g/mol Mw and 30% degree of hydrolysis (3630S in Fig. 2), permeability to oil at connate water saturation averaged 1220 md. For cores flooded with a post-hydrolyzed HPAM with 21×10^6 g/mol Mw and 30% degree of hydrolysis (6030S in Fig. 3), permeability to oil at connate water saturation averaged 250 md.

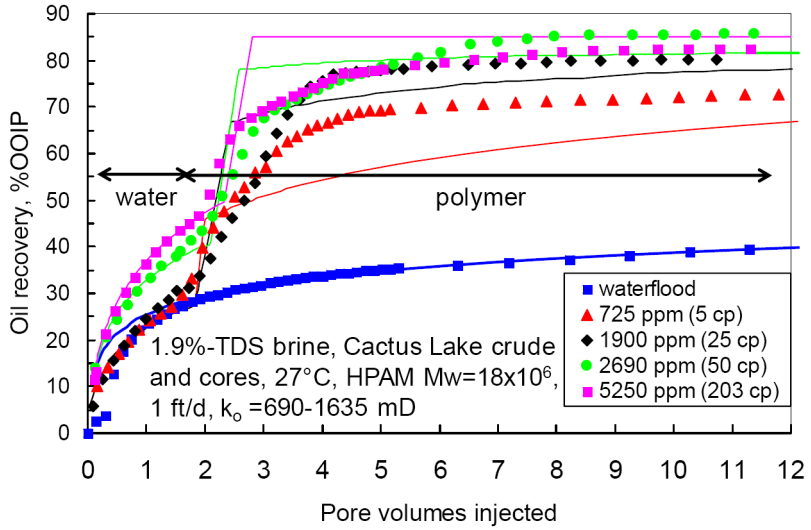

Figure 2—Oil recovery response in high-permeability field cores.

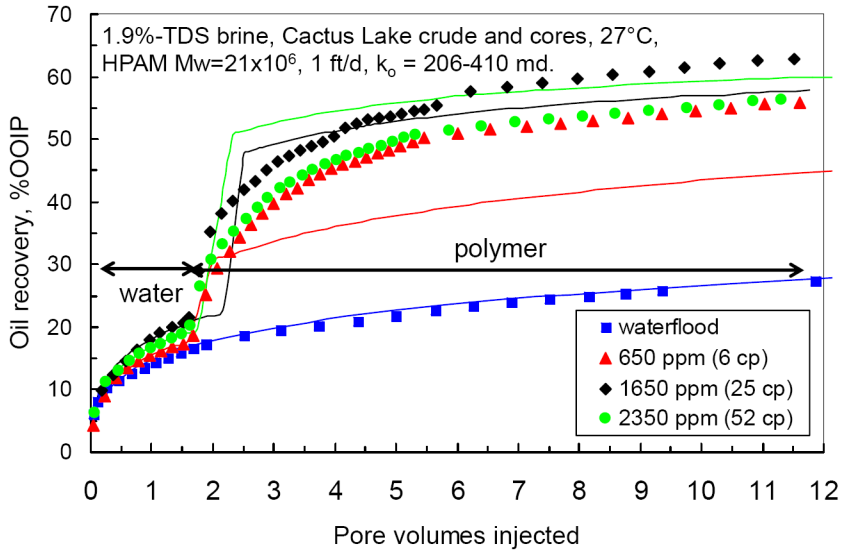

Figure 3—Oil recovery response in less-permeable field cores.

After oil saturation, ~1.5 PV of synthetic Cactus Lake brine was injected at 1 ft/d. Relative permeability to water and oil were calculated, based on continuously monitored pressure across the core, oil production, and water cut. Oil/water separations were accomplished by centrifugation and oil adherence to polyethylene sample tubes. After 1.5 PV of brine, water cuts were over 90% for all cores. In seven cores, about 10.5 PV of polymer solution were injected, followed by about 40 PV of brine. Subsequently, about 40 PV of toluene and 40 PV of methanol were injected to clean the core. Finally, the core was dried in an oven to remove the solvents. Mass balances were used to estimate remaining oil saturation (S_o) at a given stage of the experiment and to estimate the initial water saturation in the core (S_{wi}).

A dilemma exists when core flooding with viscous oils, regarding whether to flood at high or low rates. By flooding at high rates, the capillary end effect can be minimized, if the cores are water wet (Willhite 1986). In contrast, Maini (1998) proposed the use of low flooding velocities when measuring relative permeability with viscous oils to minimize complications associated with fines migration and in situ emulsification—as well as being more representative of fluid velocities in the bulk of the reservoir. Another major concern with using high rates is mobilization of residual oil and attainment of relative permeability values that would not be achievable at typical reservoir rates. This work will demonstrate that this concern is justified for

our cases (Figs. 17 and 18). A third point is that high fluid velocities could accentuate viscous fingering in water-wet cores (Peters and Flock 1981, Doorwar and Mohanty 2017). Mai and Kantzas pointed out (2010) that although capillary forces are typically thought negligible in heavy-oil reservoirs, they can be inportant and result in significiant oil recovery. Consequently, a low rate (1 ft/d Darcy velocity) was chosen for our core floods. Although measurements might be distorted by the capillary end effect near the time of water breakthrough, our interest in relative permeability is focused on measurements made well after water breakthrough. Experiments were performed with various wetting states of the field cores (native, water-saturated first, oil-saturated first) in hopes of assessing how strongly capillary forces impacted our results. Further, studies were performed in strongly oil-wet porous polyethylene cores for comparison.

Results

25-cp Polymer Appears Optimum for Oil Displacement in Corefloods

Oil recovery versus pore volumes injected is plotted in Figs. 2 and 3 for the two HPAM polymers. Tables 2 and 3 provide additional details for the cores and floods. Fig. 2 and Table 2 apply to HPAM with Mw=18 million g/mol in 690- 1635-md cores, while Fig. 3 and Table 3 apply to HPAM with Mw=21 million g/mol in 206-410-md cores. (The lower-Mw polymer used high-permeability cores simply because those experiments were performed first, and the best cores were used at that time. Later, when the higher-Mw polymer was tested, only less- permeable field cores were available.)

For a given condition, oil recovery was consistently greater in the high-permeability cores (Fig. 2) than in the less-permeable cores (Fig. 3). Waterflood responses in the four less-permeable cores (Fig. 3) were quite similar—with oil recovery values ranging from 15.9 to 20.7% original oil in place (OOIP) after 1.5 PV of water injection. For three of the more-permeable cores (blue, red, and black data in Fig. 2), waterflood responses were also similar—with oil recovery values ranging from 27.4 to 30.5% OOIP after 1.5 PV of water injection. However, two of the more-permeable cores showed noticeably higher recovery values (39.1 and 43.7% OOIP) after 1.5 PV of waterflooding (green circles and pink squares in Fig. 2).

Each of the waterflood data sets (i.e., the first 1.5 PV in Figs. 2 and 3) were fitted to Brooks-Corey equations:

$$k_{rw} = k_{rwo}\,[(S_w - S_{wi})/(1 - S_{or} - S_{wi})]^{nw} \quad (1)$$

$$k_{ro} = [(1 - S_w - S_{or})/(1 - S_{or} - S_{wi})]^{no} \quad (2)$$

Here, k_{rw} is relative permeability to water, k_{ro} is relative permeability to oil, S_w is water saturation, S_{wi} is initial water saturation, S_{or} is residual oil saturation, and nw and no are saturation exponents. (In this work, the endpoint relative permeability to oil is assumed to be one, based on oil permeability at S_{wi}.) Parameters from the fits are listed in Table 4. These values were used as input into fractional flow calculations (Seright 2010) to project oil recovery during subsequent polymer injection. In Figs. 2 and 3, each solid curve of a given color is the fractional flow projection associated with the data of that same color. Note that more than one set of parameters may provide an adequate fit. For example, waterflooding of Core 1 (top of Table 4) lists fitting parameters of S_{wi}=0.17, S_{or}=0.35, $k_{rw}o$=0.05, nw=2, and no=3. An acceptable alternative fit could be obtained using S_{wi}=0. 1, S_{or}=0.15, $k_{rw}o$=0.7, nw=3.5 and no=4.

Table 4—Fractional flow fitting parameters for Figs. 2 and 3.

Core	fluid	$k_{rw}o$	S_{wi}	S_{or}	nw	no
1	water	0.05	0.17	0.35	2	3
24	5 cp 3630	0.12	0.1	0.15	1.5	2
27	25 cp 3630	0.12	0.1	0.15	1.5	2
26	50 cp 3630	0.035	0.1	0.15	1.5	2.2
29	200 cp 3630	0.035	0.1	0.15	1.5	1
23	water	0.6	0.15	0.3	2	3
20	6 cp 6030	0.6	0.15	0.3	2	2
30	25 cp 6030	0.35	0.15	0.3	2	2
21	52 cp 6030	0.45	0.15	0.3	2	2

After injecting 1.5 PV of brine, ~10.5 PV of polymer solution was injected. For both polymers, a substantial increase in oil recovery was noted when switching from water to polymer injection (data points in Figs. 2 and 3). In the more-permeable cores (Fig. 2), fractional flow projections predicted that oil recovery should increase with increase viscosity of the injected polymer—although relatively modest differences were projected near the end of polymer injection. The data indicated the highest ultimate recovery from the 50-cp polymer solution—although ultimate recoveries for the 25-, 50-, and 203-cp polymers were not greatly different. Interestingly, the incremental recovery (over the recovery noted at 1.5 PV of waterflooding) was highest for the 25-cp polymer solution (fourth to last row in Table 2).

In the less-permeable cores (Fig. 3) after injecting ~10.5 PV of polymer solution, the 25-cp polymer solution (black diamonds) provided the highest oil recovery. Oil recovery when injecting 52-cp polymer solution (green circles) was comparable to that when injecting 6-cp polymer solution. The fractional flow projection for 52-cp polymer (green curve in Fig. 3) was modestly higher than for the 25-cp polymer (black curve).

No Reduction of S_{or}

The above observations (especially the fourth to last rows in Tables 2 and 3) indicate maximum oil recovery associated with injecting 25-cp polymer solution. One could argue that recoveries for the 25-203-cp polymer cases were similar (for a given core permeability) and that differences were simply due to core-to-core variations or due to experimental error. Nonetheless, for this particular oil and set of cores, high concentrations of high-Mw HPAM polymers did not convincingly drive the residual oil saturation below expectations from prolonged waterflooding. This result is in opposition to that observed for the Daqing polymer flood (Wang et al. 2000, 2001a, 2001b, 2010, 2011), where concentrated high- Mw polymers reportedly drove the residual oil saturation down by 15 saturation-percentage points. In Fig. 2, actual ultimate oil recoveries were slightly greater than projections for the 25- and 50-cp polymers but slightly less than projections for the 203-cp polymer. In Fig. 3, actual ultimate oil recoveries were greater than projections for the 25-cp polymer but less than projections for the 50-cp polymer.

Other observations are relevant to the current literature discussion on the effect of polymer concentration and viscosity on displacement of trapped residual oil. Since our experiments used a fixed injection rate of 1 ft/d, the capillary number when injecting 25-, 50-, and 203-cp polymer solutions should be 25-203 times higher when injecting polymer than for the previous water injection (because rate and interfacial tension were constant). Consequently, displacement of additional oil was expected with increased polymer concentration. Later (in Figs. 17 and 18), evidence of mobilization of residual oil is presented when waterflood flux increased from 1 to 16 ft/d. Since oil recovery did not increase noticeably for polymer concentrations above 25 cp (Figs. 2 and 3), the HPAM polymer solutions apparently did not mobilize trapped

residual oil for our floods. Also, note in the second to last rows in Tables 2 and 3, significant volumes of residual oil were recovered by toluene extraction at the end of the experiments. The literature observations of polymers mobilizing trapped residual oil in other applications (e.g., Daqing) are not doubted here. Our work only indicates that polymers don't mobilize trapped residual oil in our application. For many previous reports where polymer flooding apparently reduce the endpoint S_{or}, it is noteworthy that injection rates and capillary numbers were relatively high.

Additional insight into the apparent optimum associated with 25-cp polymer solutions may come from Fig. 4. This figure replots the oil recovery projections based on the parameters in Table 4. However, instead of plotting oil recovery in %OOIP (as in Figs. 2 and 3), Fig. 4 plots % of mobile oil recovered. When presented in this way, Fig. 4 shows that (except at low PV values) recovery projections bunch together (above 90% of mobile oil recovered) for polymer viscosities of 25 cp and above. This observation implies that the apparent "optimum" of 25-cp polymer noted in Figs. 2 and 3 simply reflects core-to-core variations in endpoint water and oil saturations. Put another way, if the reservoir was homogeneous with linear flow, little incremental oil would be recovered by injecting more than 25-cp polymer. The consequences if the reservoir is not homogeneous will be discussed later.

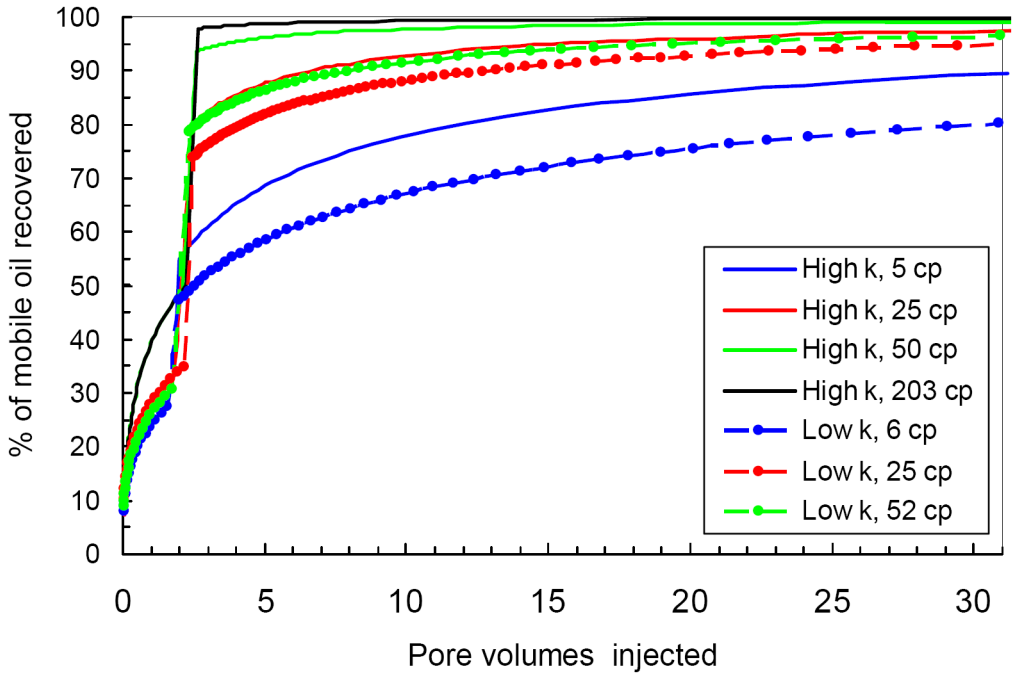

Figure 4—Replot of fractional flow projections from Table 4: % of mobile oil recovered versus PV.

Anomaly with 5-6-cp Polymer Solutions

Interestingly, in both Figs. 2 and 3, the fractional flow projections for the 5-6-cp polymer solutions (red curves) were notably below the actual polymer data points (red triangles). Vittoratos and Kovseck (2017) speculated that emulsification may be the dominant mechanism for polymer flooding of viscous oils, rather than viscosity increase. They speculate that above some minimum concentration (e.g., 3 cp), polymers may promote formation of viscous emulsions which improve the mobility ratio and provide a "self-diversion" mechanism. In the present work, the oil/water effluent did not appear to be significantly emulsified, either by water or polymer injection. For the cases tested, the aqueous effluent was not more viscous than the injected water or polymer solution. Further, the viscosity of the produced oil was the same as that for the injected oil. On the other hand, one could use the 5-6-cp HPAM data as possible support for the emulsification idea. Fractional flow calculations were performed to assess the "effective polymer viscosity" required to match the observed oil recovery values in Figs. 2 and 3. In Fig. 2, matching the 5-cp-HPAM data (red

triangles) required an assumption of 10-cp polymer during the fractional flow calculations. Matching the 25-cp-HPAM data (black diamonds in Fig. 2) required an assumption of 40-cp polymer. However, if in-situ emulsification was truly responsible for the increased apparent viscosity, it appears to be a modest effect (i.e., a factor of two or less). The emulsification concept might appear stronger when viewing the data in the less-permeable core (Fig. 3). Matching the 6-cp-HPAM data (red triangles) required an assumption of 29-cp polymer, while matching the 25-cp-HPAM data (black triangles) required an assumption of 80-cp polymer. The results in the less- permeable cores indicate a viscosity enhancement of 3-6, in contrast to the 1.6-2-fold enhancement in the more-permeable cores. If an emulsification concept is valid, this result argues against a "self-diversion" mechanism—since the "emulsion" apparently restricted less-permeable flow paths more than high- permeability flow paths.

Two other ideas will be discussed later to explain the discrepancy between the 5-6-cp recovery data and the fractional flow projections. One concept (based on the work of Doorwar and Mohanty 2017) involves reduced viscous finger to improve recovery more than would be expected from fractional flow calculations. The second idea is that resistance factors for the polymer solutions were significantly greater than expectations from viscosity measurements.

Relative Permeabilities for Field Cores

Calculations of relative permeability were made using the method of Johnson et al. (1959), as modified by Jones and Roszelle (1978). For the field cores mentioned above, during water injection, Figs. 5 and 6 plot relative permeability to water and oil, respectively. In each figure, the solid symbols (including the asterisk) refer to the high-permeability cores, while the open symbols refer to the less-permeable cores. The key result from Fig. 5 is that relative permeability to water remained low—less than 0.03 for water saturations up to 0.42. Further, relative permeability to oil remained reasonably high (greater than 0.05) for most of this range (Fig. 6). These observations help explain why only 25-cp polymer solutions were effective in recovering 1610-cp oil. The low relative permeability to water (<0.03) allowed 25-cp polymer to provide close to a favorable mobility ratio. At the same time, the relatively high relative permeability to oil (> 0.05) allowed oil behind the water front to continue flowing at a reasonable rate.

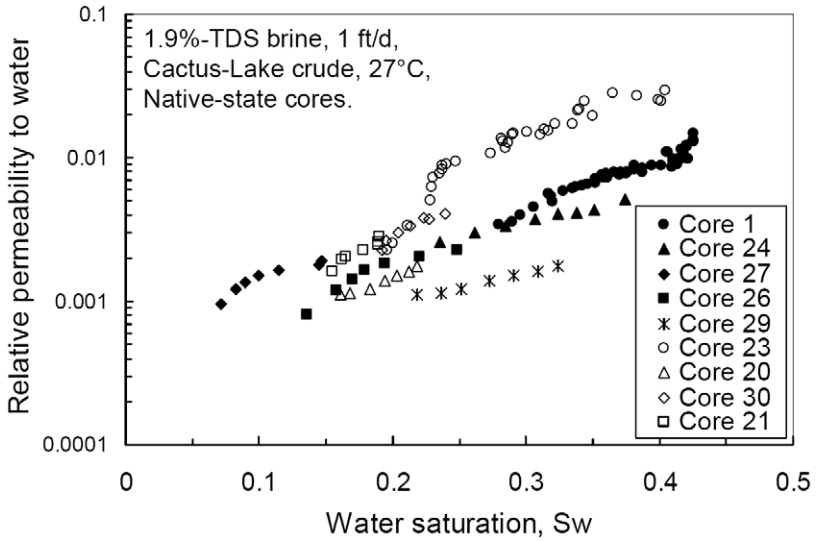

Figure 5—Relative permeability to water for field cores.

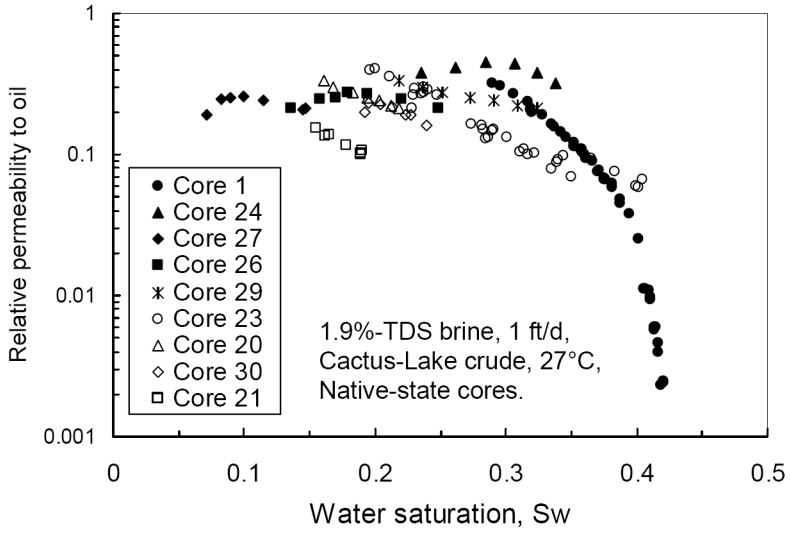

Figure 6—Relative permeability to oil for field cores.

Maini (1998) reviewed the challenges associated with measuring relative permeability for heavy oil reservoirs. He pointed out that damage to cores can affect relative permeabilities—especially since debris or permeability reductions on core faces can have a substantial impact. In our cases, inspection of core faces and use of filtered fluids were hoped to minimize this effect. However, the possibility of core damage cannot be exclude. It is possible that this effect could explain some of the differences in relative permeability curves seen in Figs. 5 and 6.

Maini (1998) and Huh and Pope (2008) noted that core heterogeneity can accentuate viscous fingering/channeling through cores that affects recovery efficiency—and consequently affects the measurements of relative permeability. For two cases (Field Core 1 and Polyethylene Core 1), tracer studies were performed on cleaned, oil-free cores (using the method described in Seright and Martin 1993). In both cases, tracer breakout curves were very sharp with no tailing—indicating homogeneous cores.

When calculating relative permeability in Figs. 5 and 6, capillary pressure was neglected. Maini (1998) discussed the problems with this assumption. Because our experiments were conducted at a low rate, capillary pressure effects may have distorted the relative permeability values near the time of water breakthrough—if the cores were water wet. This concern will be addressed shortly by performing experiments with different sequences of core saturation and by using cores that are strongly oil wet. Also, as mentioned earlier, our primary interest in relative permeability focusses on the time well after water breakthrough.

Effect of Saturation History, Oil, and Oil Viscosity

A key result from the above studies was that injection of 25-cp polymer solution appeared optimum for displacement of 1610-cp oil from the field cores. Was this result due to the saturation history, the nature of the oil, or the oil viscosity?

Field Core 1 was subjected to extended (30 PV) water injection during additional studies of saturation history and nature of oil used for saturation. In the first experiment, the core was received in its native state, saturated with crude oil, and flooded with brine—just as with the other field cores mentioned above (except that 30 PV of brine was injected in Core 1). After 30 PV of brine injection, the core was flushed with 40 PV of toluene, followed by 40 PV of methanol to clean the core. Then the core was dried. For the second experiment, the cleaned core was saturated with brine, followed by saturation with crude oil, then 30 PV of brine, and cleaning as in the first experiment. The third experiment was identical to the second, except that the core was first saturated with oil instead of brine. The fourth experiment was identical to the second, except that the oil was Soltrol 170—a refined oil with a viscosity of 2.9 cp at 27°C. The fifth experiment

was identical to the second, except that the oil was Cannon S600—a refined oil with a viscosity of 1000 cp at 27°C.

During the course of injecting 30 PV of brine, Figs. 7-9 plot oil recovery, relative permeability to water, and relative permeability to oil, respectively. Table 5 lists relative-permeability fitting parameters associated with the curves in Fig. 7. As expected, oil recovery was very efficient when brine displaced 2.9-cp oil, relative permeability to water rapidly approached the endpoint value of 0.24, and relative permeability to oil rapidly dropped to low values (Figs. 7, 8, and 9, respectively). Also, as expected, displacement efficiency was substantially lower for the 1000-cp oils than for the 2.9 cp oil. Fig. 7 shows that displacement of 1000-cp oil was most efficient for the refined S600 oil (black diamonds) in the cleaned core and least efficient for the crude oil in the native-state core (red circles). Displacement efficiencies were similar for the cleaned cores that were first saturated with water (blue triangles in Fig. 7) and that were first saturated with crude oil (green squares). For the various cases using 1000-cp oils, relative permeability to oil showed considerable scatter and similar behavior, within the experimental error (Fig. 9). (The data scatter for k_{ro} occurred because oil drops were produced erratically at high water cuts.)

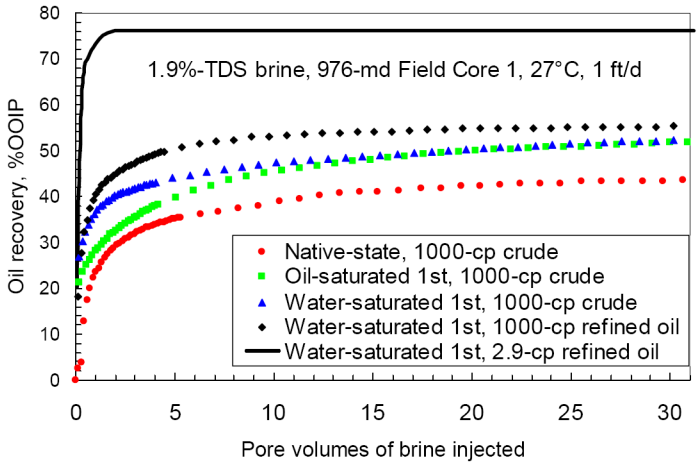

Figure 7—Oil recovery versus PV for Core 1.

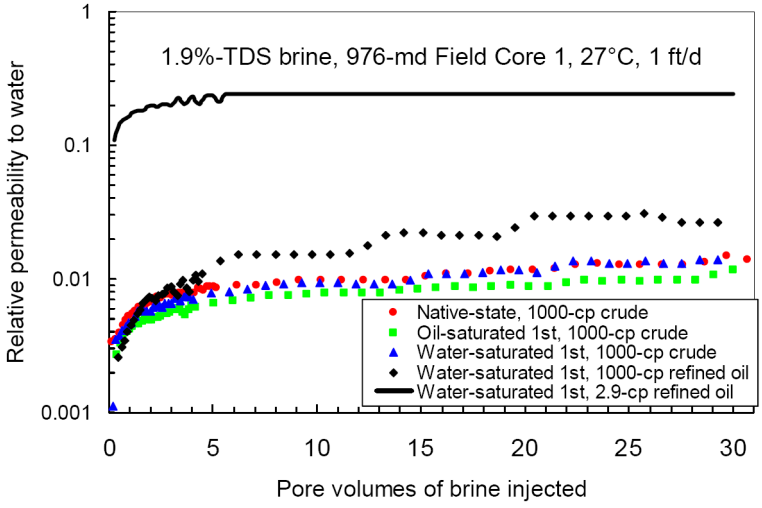

Figure 8—Relative permeability to water versus PV for Field Core 1.

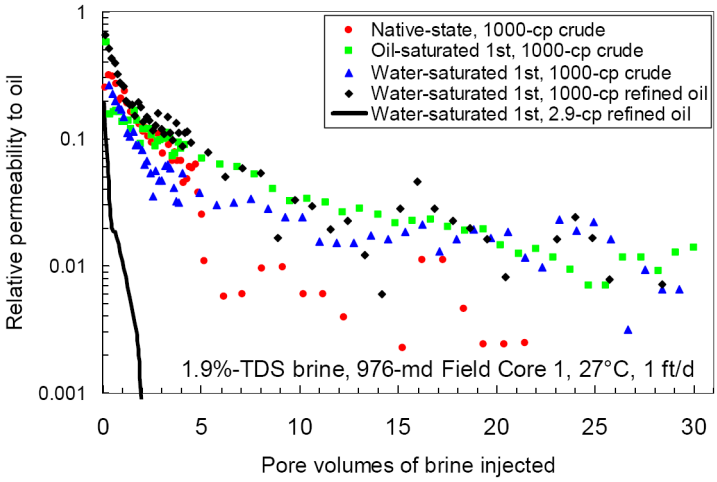

Figure 9—Relative permeability to oil versus PV for Field Core 1.

Table 5—Fractional flow fitting parameters for Fig. 7 (Field Core 1).

Saturation history	Oil	Oil viscosity, cp	k_{rwo}	S_{wi}	S_{or}	*nw*	*no*
Native state	Crude	1000	0.05	0.17	0.35	2	3
Water 1st	Crude	1000	0.09	0.1	0.15	2.3	4
Oil 1st	Crude	1000	0.09	0.1	0.15	2.3	4
Water 1st	Cannon S600	1000	0.05	0.1	0.15	4.4	5
Water 1st	Soltrol 170	2.9	0.24	0.1	0.2	1.5	1.7

Fig. 7 demonstrates that oil recovery was inefficient for all four cases involving water displacement of 1000-cp oil. The relative permeability to water was low after 30 PV of brine injection—ranging from 0. 014 to 0.035 for the 1000-cp-oil cases. In examining the fits to the oil recovery curves (Fig. 7 and Table 5), the assumed endpoint $k_{rw}o$ values were not unusually low (0.05 to 0.09). Thus, although the saturation history and oil nature (refined versus crude) can impact displacement efficiency, their effects do not substantially alter the inefficient nature of water displacing 1000-cp oil.

For Field Core 1, Figs. 10 and 11 plot relative permeability to water and oil, respectively, versus water saturation. Relative permeability to water showed similar shapes and trends for all four cases with 1000-cp oil—including the 1000-cp refined oil (black diamonds in Fig. 10). However, the k_{rw} curves shifted with water saturation. The k_{rw} curve associated with the native-state core (perhaps the most oil wet?) was shifted most toward low water saturations, while the curve associated with the 1000-cp refine oil (probably the most water wet) was shifted most to high water saturations. The k_{rw} curve for the 2.9-cp refined oil (pink triangles in Fig. 10) could be viewed as an extension of the trend associated with the 1000-cp oils. As with the other field cores (Fig. 5), values for k_{rw} remained below 0.03 for much of the testing (up to water saturations of 0.63 for 1000-cp refined oil).

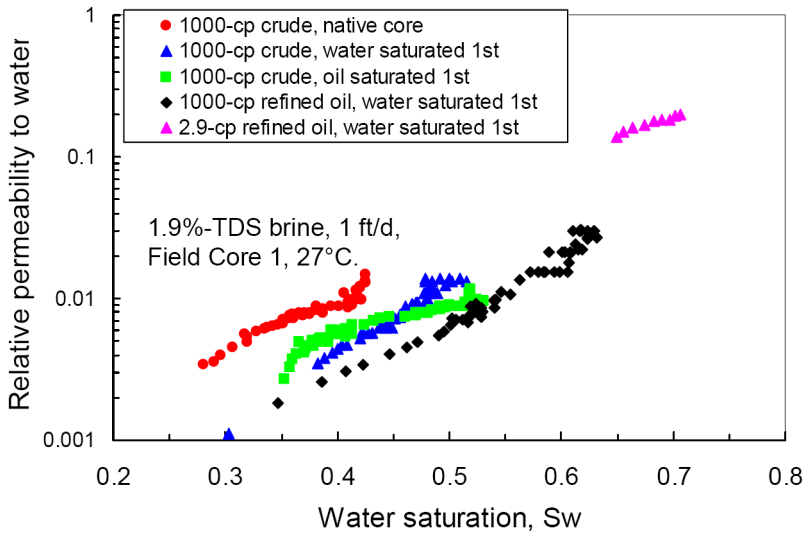

Figure 10—Relative permeability to water versus S_w for Field Core 1.

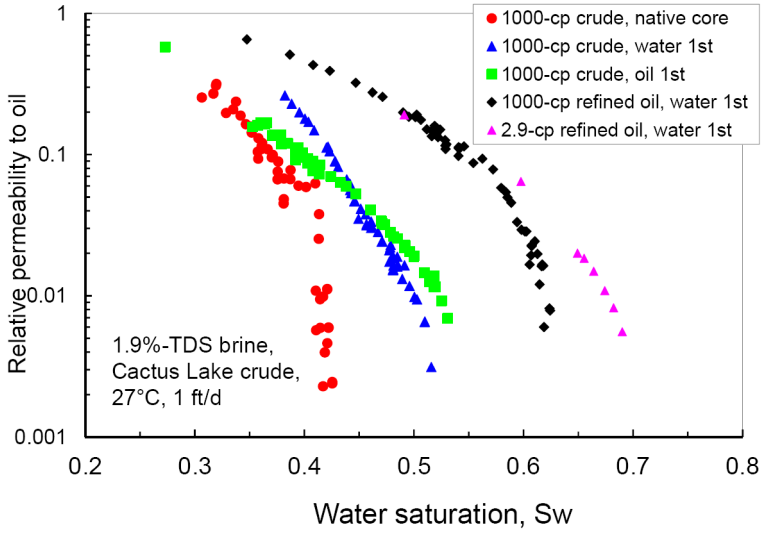

Figure 11—Relative permeability to oil versus S_w for Field Core 1.

In Fig. 11, relative permeability to oil exhibited similar shapes and trends for all five oils. Again, the curves showed significant shifts with water saturation. The three crude-oil k_{ro} curves were somewhat close together, while the two refined-oil k_{ro} curves were shifted to higher water saturations. In all five cases, k_{ro} remained above 0.05 for a significant range of saturation—just as was noted for Fig. 6.

Behavior in Porous Polyethylene Cores

The field cores used in the previous sections contained about 85% quartz or feldspars, 10% iron oxide, and 2.5% clay (mostly kaolinite). This section describes core floods in porous polyethylene cores. These cores are described in Seright et al. (2006) and have a pore structure (pore size distribution, pore throat distribution) that is similar to Berea sandstone. However, grain surfaces are quite smooth, in contrast to the rough appearance of clays on quartz grains (Seright et al. 2006). As expected, the porous polyethylene cores were strongly hydrophobic and exhibited very high contact angles with all oils tested (i.e., those in Table 1).

Five waterfloods were performed in a single porous polyethylene core using five different oils (Table 1). The core was 3.81-cm in diameter and 6.27-cm long, with a porosity of 0305, absolute permeability of 2000 md, and pore volume of 21.8 cm^3. As with the previous cores, the experiments were performed at 27°C

and an injection flux of 1 ft/d. The overburden pressure was 200 psi. In the first experiment, the core was saturated with brine, flooded with 4 PV of 2.9-cp Soltrol 170 oil, and then flooded with 30 PV of brine. The core was then flooded with 4 PV of 28-cp Cannon S20 oil in preparation for the second experiment—where 30 PV of brine was injected. This procedure was repeated using 130-cp Equate mineral for the third experiment, 1000-cp Cannon S600 oil for the fourth experiment, and 1000-cp Cactus Lake crude for the fifth experiment. Results are shown in Figs. 12-14.

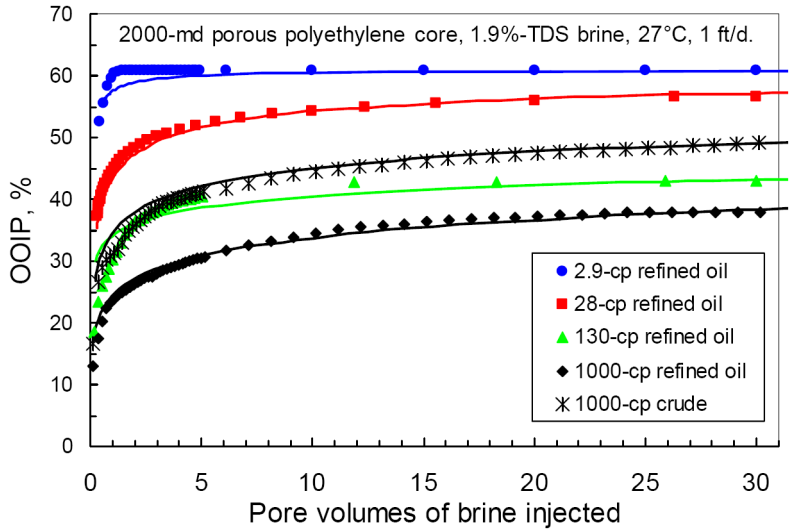

Figure 12—Oil recovery in a polyethylene core versus oil viscosity.

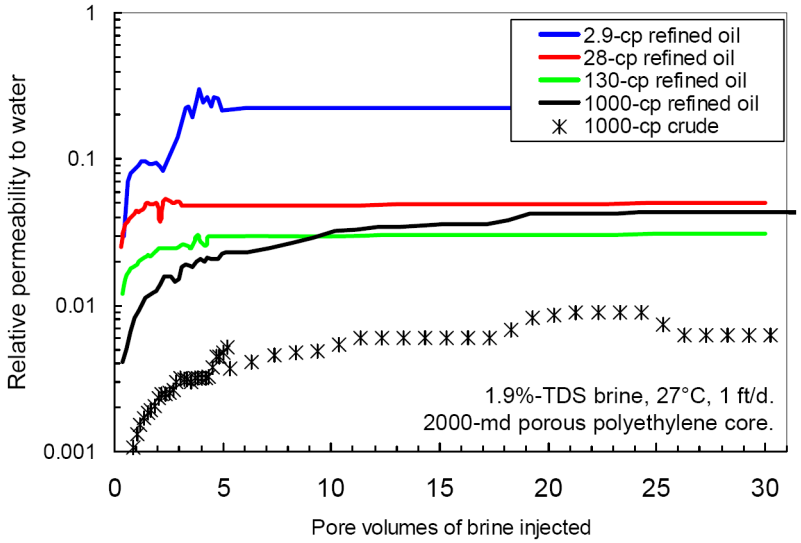

Figure 13—k_{rw} in a polyethylene core versus oil viscosity.

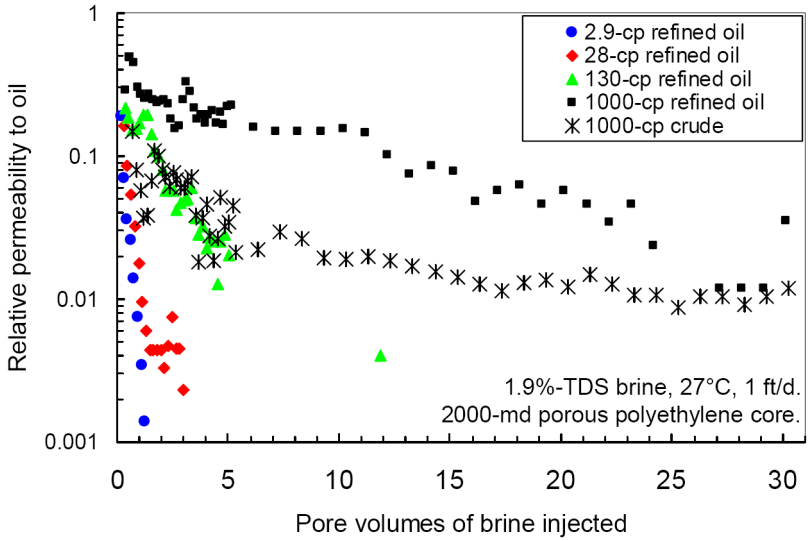

Figure 14—k_{ro} in a polyethylene core versus oil viscosity.

Fig. 12 shows waterflood recovery efficiency for the five oils. The data points of a given color show the actual recovery values at a given PV, while the solid curves of that color show the fit to Eqs. 1 and 2 using the parameters in Table 6. For the refined oils, a good fit was obtained for all refined oils using S_{wi}=0.18, S_{or}=0.32, k_{rwo}=0.24, and kroo=1. For the crude oil, a much lower k_{rwo} value (0.02) was needed. For the refined oils, at a given brine PV throughput, oil recovery decreased with increase oil viscosity, as expected. However, surprisingly, oil recovery with the 1000-cp crude oil was higher than expected— exceeding that for the 130-cp mineral oil.

Table 6—Fractional flow fitting parameters for Fig. 12 (Polyethylene Core 1).

Oil	Oil viscosity, cp	k_{rwo}	S_{wi}	S_{or}	*nw*	*no*
Soltrol 170	2.9	0.24	0.18	0.32	4	2
Cannon S20	28	0.24	0.18	0.32	2.7	2.5
Equate mineral oil	130	0.24	0.18	0.32	5.5	5.5
Cannon S600	1000	0.24	0.18	0.32	3.4	3.4
Crude	1000	0.02	0.18	0.32	3	3.5

Fig. 13 plots relative permeability to water for the five oils. At a given PV, relative permeability to water was quite high (~0.24) for the refined 2.9-cp oil. For the 28-, 130-, and 1000-cp refined oils, the relative permeabilities to water after 10 PV of brine were similar—in the range from 0.02-0.04. Interestingly, k_{rw} values associated with the 1000-cp crude oil were 3-10 times lower than for the 28-1000- cp refined oils. This effect appears to be responsible for crude oil recovery being higher than oil recovery associated with the 130-cp oil (Fig. 12).

Fig. 14 plots relative permeability to oil for the five oils. Interestingly, the curve for the 1000-cp crude was more similar to that for the 130-cp mineral oil than for the 1000-cp refined oil. The case with 1000- cp refined oil maintained the highest k_{ro} values for the highest PV throughputs.

Figs. 15 and 16 plot relative permeability versus water saturation. The refined oils exhibited similar k_{rw} and k_{ro} behavior. Although modest deviations were noted (especially for the 2.9-cp refined oil), the relative permeabilities (for both k_{rw} and k_{ro}) followed about the same behavior for all four refined oils (with viscosities of 2.9-, 28-, 130- and 1000-cp). Relative permeability to oil (Fig. 16) for the 1000-cp crude oil was also similar to that for the refined oils. In contrast, the relative permeability to water for the crude oil

(Fig. 15) was about ten times lower than for the refined oils (for a given water saturation). As mentioned earlier, the lowest k_{rw} values for the 1000-cp crude oil explain the relatively high recovery seen in Fig. 12.

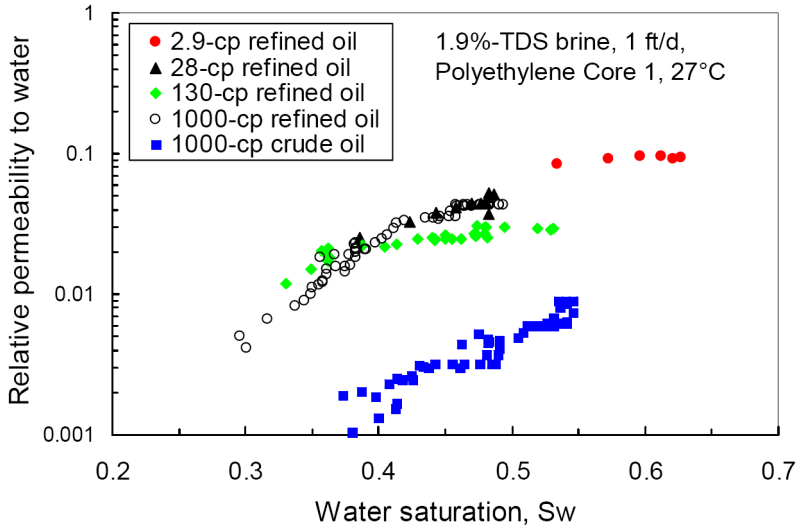

Figure 15—k_{rw} in a polyethylene core versus water saturation.

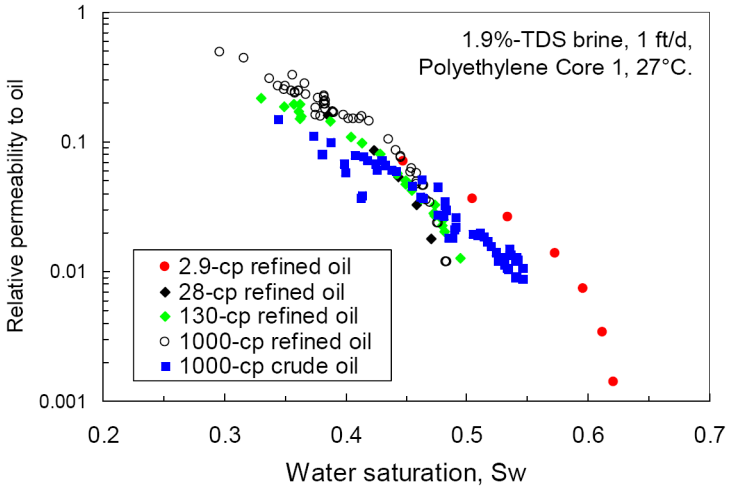

Figure 16—k_m in a polyethylene core versus water saturation.

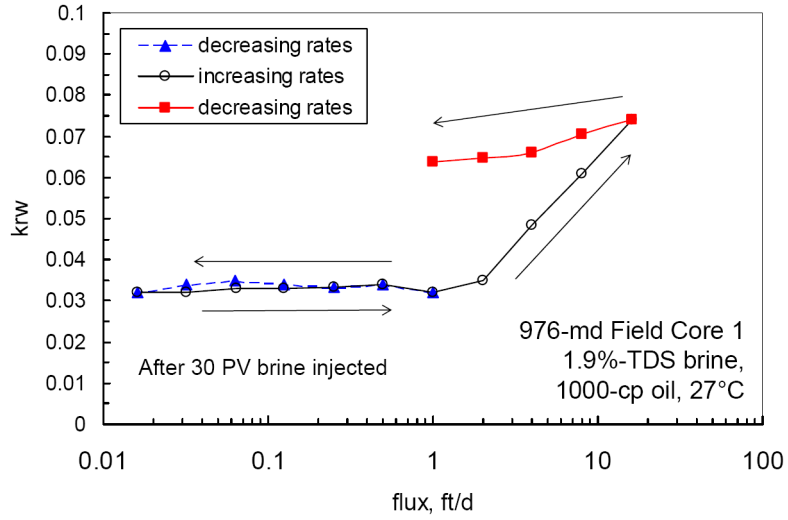

Figure 17—Effect of injection flux on k_w in Field Core 1 after 30 PV.

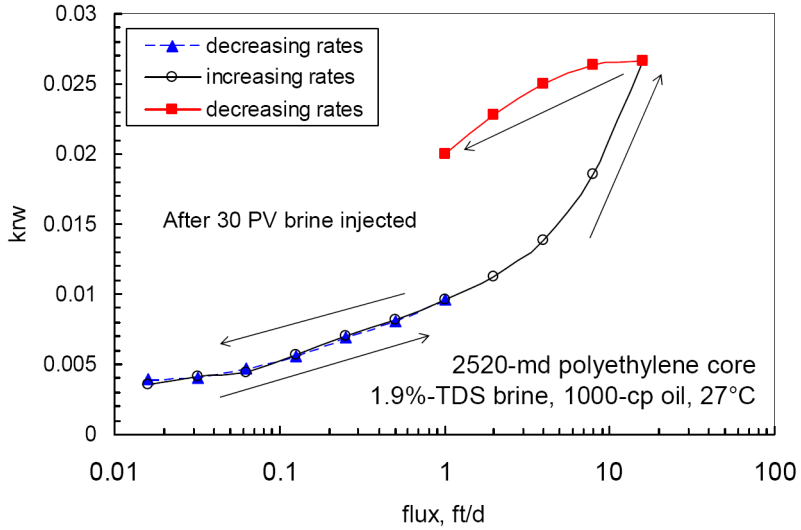

Figure 18—Effect of injection flux on k_w in a polyethylene core after 30 PV.

Previous literature is qualitatively consistent with our observations. With a few exceptions, much of the literature indicates that relative permeability behavior is not sensitive to oil viscosity—although it is sensitive to wetting behavior (Willhite 1986). Sandberg et al. (1958) found that relative permeability to oil or water was not affected by oil viscosity (for refined oils) between 0.398 and 1.683 cp in 4-6-inch-long sandstone cores. In a 1-ft-long 325-200-mesh sand packs, Richardson (1957) found that the ratio of k_{rw} / k_{ro} was the same for 1.8-cp kerosene and 151-cp oil (of unspecified origin). Odeh (1959) presented a controversial paper where he noted that the apparent relative permeability to oil increased dramatically with increased oil viscosity at relatively low water saturations. However, at higher water saturations, his relative permeabilities appeared more in line with the above literature (i.e., not sensitive to oil viscosity). Wang et al. (2006) studied crude oils with viscosities ranging from 430 to 13,550-cp in 5.6-in long, 1.67in diameter, 100-60-mesh Ottowa sand packs. They reported that both relative permeability to both water and oil decreased significantly with increased oil viscosity in the water saturation range between 40% and 60%. However, a close look at their data revealed that their k_{rw} and k_{ro} values were insensitive to oil viscosity from 430 to 1860 cp. Substantial differences were only seen for oil viscosities of 5410 cp and above.

Effect of Fluid Velocity

For two experiments, after injecting 30 PV of brine to displace 1000-cp oil, the water injection rate was varied to examine the effect on the relative permeability to water. One experiment was performed in Field Core 1 (Fig. 17) while the other was performed in a 2520-md porous polyethylene core (Fig. 18). In both cases, the experiment started with an injection flux of 1 ft/d. After stabilization, the pressure was recorded and k_{rw} was calculated. Then the rate was cut in half, and stabilization was again allowed. This procedure was repeated using successively lower rates, down to a flux of 0.016 ft/d (blue triangles in Figs. 17 and 18). Next, the flux was doubled in stages up to a maximum of 16 ft/d (open circles in Figs. 17 and 18). Finally, the flux was again halved in stages back to a value of 1 ft/d (red squares in Figs. 17 and 18).

In Field Core 1 (Fig. 17), k_{rw} was independent of flux between 1 ft/d and 0.016 ft/d—regardless of whether rates were decreasing or increasing. Since the measurements were made over the course of a relatively small throughput (0.8 PV), no significant changes in water saturation occurred, so a constant k_{rw} was expected. As flux was raised from 2 ft/d to 16 ft/d, k_{rw} rose from 0.032 to 0.074. This increase in k_{rw} was attributed to increased oil mobilization associated with raising the capillary number. When the rates were subsequently decreased from 16 ft/d to 1 ft/d (red squares), k_{rw} values remained above 0.063— consistent with mobilization and reduction of residual oil. A similar behavior was noted in a porous polyethylene core (Fig. 18), except that a reversible velocity effect was noted on k_{rw} for flux values between 0.016 and 1 ft/d.

Discussion and Relevance to Field Applications

Consistency with Previous Literature

Several researchers reported results of corefloods where polymer solutions displaced heavy oil. Asghari and Nakutnyy (2008) used an unspecified polyacrylamide (concentrations from 500 to 10000 ppm in 1%-TDS brine) to displace either 1000-cp or 8400-cp oils from either 2.1 D or 13 D sand packs. As expected, oil recovery was significantly higher when flooding packs containing 1000-cp oil than for packs containing 8400-cp oil. For a given polymer concentration and oil viscosity, oil recovery was modestly higher as rate decreased from 50-ft/d to 1 ft/d—possibly indicating a small reduction in viscous fingering associated with capillary effects in water-wet packs. Surprisingly, they found that oil recovery increased only slightly as polymer concentration was raised from 0 ppm (i.e., waterflooding) to 1000 ppm. Oil recovery did increase noticeably as polymer concentration increased from 5000 to 10000 ppm. Viscosity of the polymer solutions were not specified, but the results suggest that viscosity and polymer molecular weight may have been low compared to current HPAM solutions that are commercially used for polymer flooding. The requirement of at least 5000-ppm polymer to mobilize significant oil argues against the emulsification mechanism proposed by Vittoratos and Kovscek (2017). If HPAM is sufficiently interfacially active to promote emulsification, one might expect emulsification to occur with much less than 5000-ppm polymer.

Wang and Dong (2008) studied polymer flooding of homogeneous and "heterogeneous" sand packs that were saturated with 1450-cp oil. Results from their studies were qualitatively consistent with conventional expectations for polymer flooding. First, in both homogeneous and heterogeneous sand packs, oil recovery improved monotonically with increased polymer viscosity (from 2.1 cp to 76.3 cp). Second, oil recovery was ultimately greater/more efficient in homogeneous packs than in heterogeneous packs.

Beyond the above observations that are consistent with accepted polymer flooding concepts, a statement was made by Wang and Dong that could be interpreted differently, depending on the reader. First, they said "There existed a lower limit and an upper limit of the effective viscosity of polymer solution" (for effectively displacing oil). On the surface, this statement is not necessarily inconsistent with conventional mobility ratio concepts—as demonstrated by Figs. 7.6-7.8 of Craig (1971). If the polymer/oil mobility ratio is low and the porous medium is homogeneous, a mobility ratio of 0.01 is not any more effective than 0.1 in displacing oil. (Put another way, if all the mobile oil has been displaced, there is little point in injecting more

polymer.) At the other end, if the polymer/oil mobility ratio is high and the reservoir is very heterogenous, poor sweep efficiency results whether the mobility ratio is 10 or 100. (Of course, mobility ratio concepts predict that sweep efficiency would improve effectually if the mobility ratio was reduced to a sufficiently low value.) The data of Wang and Dong (2012) and our data do not support the speculation from Vittoratos and Kovscek (2017)—that "the efficacy of polymer flooding is independent of polymer concentration after it exceeds the minimum value needed to support emulsification of water into the oil."

Fabbri et al. (2014) observed that a 70-cp polymer solution was reasonably effective at displacing a 5500-cp oil, especially when applied after waterflooding. Skauge et al. (2014) and Loubens et al. (2017) demonstrated the value of fingering patterns developed durng waterflooding in aiding viscous oil displacement during subsequent polymer flooding.

Levitt et al. (2013) performed polymer floods (2 PV at 2 ft/d) in either 2-darcy Bentheimer cores or 5-darcy silica sand packs, displacing a 2000-cp oil. Prior to polymer flooding, at least 5 PV of water were typically injected. As with our current experiments, Levitt matched the waterflood performance using Eqs. 1 and 2. Using these matches, they found that fractional flow projections were in rough agreement with the experimental results of a 60-cp HPAM flood. They also found that a 3-cp HPAM solution was surprisingly effective in displacing oil. (This result was consistent with our findings with 5-6-cp polymer displacing 1000-cp oil in Figs. 2 and 3.) Levitt speculated several possible explanations, including (1) adsorbed polymer in throats overcoming capillary pressure necessary to mobilize trapped oil, (2) oil emulsification, (3) induction of elongational shear at the surface of viscous fingering, and (4) reduction of residual oil within the fingers. Levitt et al. pointed out that polymer retention can severely restrict the application of low-concentration polymer flooding. Much of their paper focused on stability criterial for viscous fingering. Using a number of published criteria for viscous stability, Levitt noted that most previous laboratory corefloods using viscous oils are in the "transition region"—where oil recovery is sensitive to core diameter.

Doorwar-Mohanty Analysis

The analysis of Doorwar and Mohanty (2017) provides an interesting means to view our data. They propose a dimensionless scaling factor, N_I, to predict unstable displacements.

$$N_I = (v_w \mu_w / \sigma) (\mu_o / \mu_w)^2 (D^2/k) \quad (3)$$

Where v_w is interstitial fluid velocity, μ_w is water viscosity, μ_o is oil viscosity, σ is oil-water interfacial tension, D is core diameter, and k is permeability. Viscous fingering should be more severe as N_I increases. They used this parameter to correlate with oil recovery at water breakthrough, as shown in Fig. 19. Luo et al. (2017a) applied this approach during reservoir simulations.

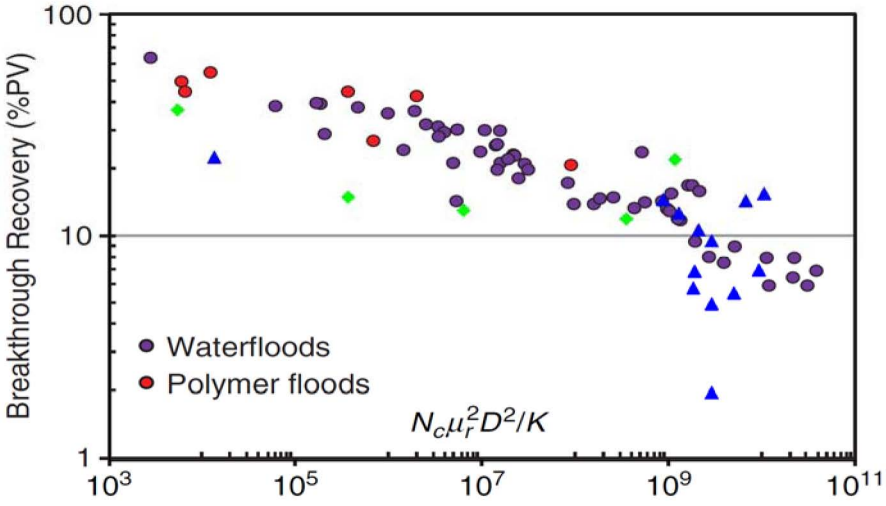

Figure 19—Plot from Doorwar and Mohanty (2017).Blue triangles are our waterflood data in field cores. Green diamonds are our waterflood data in polyethylene cores.

Some concepts from the development of this equation [and previous correlations, such as from Peter and Flock (1981)] are: (1) immiscible viscous fingering makes the displacement worse than predicted by Buckley Leverett analysis (using the "true" Brooks-Corey relations), (2) viscous fingering should be much worse in most field applications (waterflooding heavy oils) than in lab core floods because the porous-medium dimensions (effectively D^2 in Eq. 3) are much larger, and (3) attempts to measure a set of "true" relative permeability curves can be distorted (a) if the porous-medium dimensions (e.g. D^2 in Eq. 3) are too large, (b) if the oil/water viscosity ratio is too high, and (c) if the velocity is too high and the core is water wet.

For the waterfloods in Figs. 2 and 3 (in this paper), the Doorwar-Mohanty N_I (Eq. 3) is between 10^9 and 10^{10}. The blue triangles and green diamonds in Fig. 19 show that water breakthrough values from our work fall more or less in line with the correlation from Doorwar and Mohanty—although our data from the oil-wet polyethylene cores (green diamonds) generally fall below the water-wet-core data of Doorwar and Mohanty. Doorwar and Mohanty introduced a model whereby a parameter, λ, characterized the fraction of the cross-sectional flow area that was occupied by a viscous water finger in an oil zone. So λ ranged from 0 to 1. In their model, the "pseudo" or measured relative permeability to water equals λ times the "true" relative permeability to water (i.e., if no viscous fingering occurred). Thus, if significant viscous fingering occurs (as is suggested by the blue triangles in Fig. 19), the measured relative permeability to water is significantly less than the "true" or finger-free value. That concept is qualitiatively consistent with the low k_{rw} values in Figs. 5, 10, and 15. The model of Doorwar and Mohanty also predicts that the "pseudo" or measured relative permeability to oil may be higher than the "true" value because a significant amount of oil flow comes from outside the region of water fingering (where $k_{ro} \approx 1$). That prediction is also qualitiatively consistent with our relatively high k_{ro} values in Figs. 6, 11, and 16.

The concepts from Doorwar and Mohanty may qualitatively help explain why low-viscosity polymer [5-6-cp cases in Figs. 2 and 3 and the 3-cp case from Levitt et al. (2013)] provided a better displacement than projected from fractional flow calculations. The "pseudo relative permeability curves" measured during water flooding were influenced by viscous fingering—resulting in a lower oil recovery than would be predicted by "true" relative permeability curves. By injecting 5-6-cp polymer, the N_I parameter was driven to lower values in Fig. 19—resulting in less viscous fingering AND normal fractional flow improvement from injecting viscous polymer. The combination of both factors makes it appear that oil recovery was higher than expected from fractional flow projections for polymer flooding (the 5- and 6-cp projections in Figs. 2 and 3).

Continuing the interpretation, the reason that 25 cp-polymer recovered as much oil as 200-cp (in displacing 1000-cp oil in Figs. 2 and 3) was that with 25-cp polymer, no viscous fingering or channeling occurred AND the fractional flow projections were close to "topping out" on oil recovery. (This observation also confirms that the trapped residual oil saturation was not driven below expectations from infinite waterflooding). However, the observation does not necessarily indicate that 25-cp is the best choice for a field application. The dimensions of the field application (width × height or the D^2 term in Eq. 3) make viscous fingering much more likely than in the lab. Of course, heterogeneity/permeability contrast will also accentuate "fingering or channeling". The field applications should require at least as viscous of polymer as required in the lab corefloods.

The above arguments are qualitative. To quantify predictions using the Doorwar-Mohanty concepts, Luo et al. (2017b) developed an expanded fractional flow analysis. Their analysis was applied to the 5- cp-polymer flood in Fig. 2 and the 6-cp-polymer flood in Fig. 3. For our cases, predictions made using the analysis of Luo et al. (red and black asterisks in Fig. 20) were not greatly different from the standard fractional flow analysis (red and black solid curves in Fig. 20). Thus, an alternative explanation is needed for the observed oil recovery data in Figs. 2 and 3 for the 5-cp and 6-cp polymer solutions.

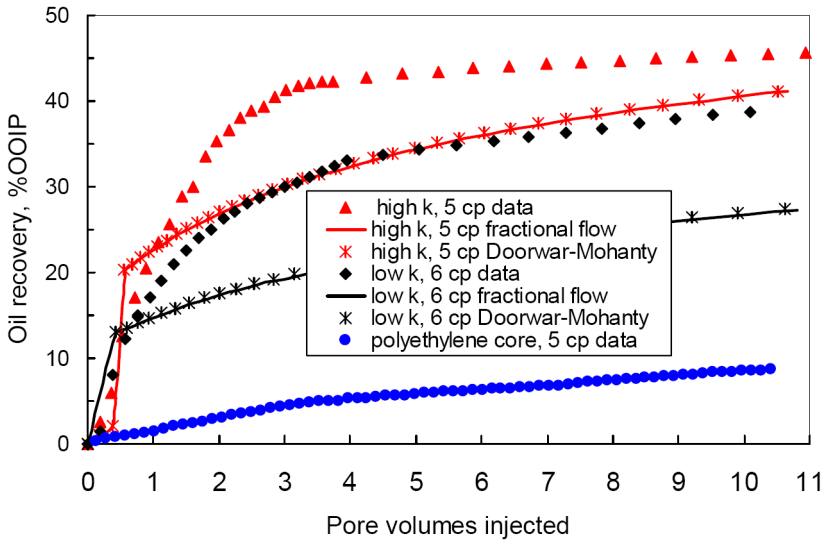

Figure 20—Oil recovery injecting 5-6-cp polymer after 1.5 PV of water.

In Situ Emulsion Formation

The issue of in situ emulsion formation was discussed earlier. As mentioned, Vittoratos and Kovseck (2017) speculated that emulsification may be the dominant mechanism for polymer flooding of viscous oils, rather than viscosity increase. Although we cannot exclude the possibility that emulsion flow led to higher than expected oil recovery for our 5-6-cp polymer solutions (red triangles and curves in Figs. 2 and 3), the emulsification mechanism is not convincing in view of our results. No signs of emulsified oil or water were noted during our experiments. Also, as Maini (1998) pointed out, emulsification is normally expected at velocities greater than present in the bulk of most reservoirs. Our experiments were conducted at a low flux of 1 ft/d, which should reduce the probability of in situ emulsification. So again, an alternative explanation is needed for the observed oil recovery data in Figs. 2 and 3 for the 5-cp and 6-cp polymer solutions.

Higher than Expected Resistance Factors

A viable explanation for the observed data is that the resistance factor for the 5-cp polymer solution in Fig. 2 was twice as high as the viscosity would suggest. Recall earlier that an assumption of 10-cp for the polymer solution for the fractional flow projections to match the 5-cp polymer data in Fig. 2. Similarly, as mentioned

earlier, an assumption of 29-cp for the polymer solution was required for the fractional flow projections to match the 6-cp polymer data in Fig. 3—meaning that the resistance factor was about 5 times greater than the viscosity. This behavior is consistent with previous observations. Seright et al. (2011) noted that freshly prepared HPAM solution can provide resistance factors that are notably greater than viscosities. The high-Mw polymer species that causes this effect is destroyed by a modest amount of mechanical degradation or by flow through a short distance of porous rock (Seright et al. 2011). Thus, this resistance factor effect cannot be expected to penetrate very far into a reservoir. Further, higher-Mw HPAMs are more likely to plug (exhibit high resistance factors and residual resistance factors) cores as the permeability decreases—consistent with a 21-million g/mol polymer providing a resistance factor five times greater then viscosity in 206-md rock while an 18-million g/mol polymer provided a resistance factor two times greater then viscosity in 1142- md rock. Additional studies of this effect can be found in Wang et al. (2008) and Guo (2017).

The most effective way to confirm this explanation would be to first force a volume of 5-6-cp polymer solution through a long field core (as was done in Seright et al. 2011) and then displace crude oil from a separate core. Unfortunately, our supply of field cores was too limited for this approach. As an alternative, a 5-cp polymer flood was performed in a 2380-md polyethylene core (after a 1.5-PV waterflood). This approach assumes that HPAM retention will be much lower in the hydrophobic polyethylene core than in the quartzitic field cores—leading to resistance factors and oil recovery values in the polytheylene cores that are much closer to expections from the 5-cp polymer viscosity. The blue circles in Fig. 20 show results from the 5-cp HPAM flood displacing 1000-cp crude oil from the 2380-md polyethylene core. Consistent with the proposed hypothesis, the oil recovery displacement shown by the blue circles was considerably less efficient than in the field cores. Also, consistent with expectations, polymer retention in the polyethylene core was substantially lower than in the quartzitic field cores. In the polyethylene core, polymer was detected in the core effluent within 0.13 PV of starting injection of 5-cp HPAM. In contrast, for the field cores, polymer was not detected in the effluent until one PV of polymer.

During flooding of viscous oils, mobility ratio is critically important—not only because of the standard Buckley-Leverett ideas, but also because the "stability equations" of Doorwar and Mohanty (and Peters and Flock and others) have mobility ratio strongly built into them (see Eq. 3).

Relevance to Field Applications

Although 25-cp HPAM solutions effectively displaced 1000-1610-cp oil during core floods, 25-cp is not nessarily sufficient for a field application. As noted by Peters and Flock (1981) and Doorwar and Mohanty (2017), the flow area in a field application is tremendously larger than in a core flood—thus radically accentuating the opportunity for viscous fingering if the mobility ratio is unfavorable. Further, reservoir heterogeneity and the potential for crossflow between layers can greatly accentuate the need for higher polymer viscosities when mobility ratios are unfavorable (Craig 1971, Sorbie and Seright 1992, Seright 2010, Seright 2017).

Previous work (Seright 2010, 2017) indicated that the ideal polymer solution viscosity for maximizing sweep efficiency in a polymer flood is different for reservoirs with single zones versus multiple zones and with no crossflow versus multiple zones with crossflow. If the reservoir can be considered a single zone with uncorrelated permeability variations, then the optimum polymer viscosity would lower the water/oil mobility ratio to near one. The same polymer viscosity is optimum for reservoirs with multiple zones but no crossflow between zones. These are the conditions present in the Cactus Lake reservoir. Since the present work demonstrates that 25-cp polymer provides a mobility ratio close to unity, 25 cp appears to be the appropriate viscosity for polymer flooding in this reservoir. In reservoirs with distinct layers and free crossflow between layers, the ideal viscosity is estimated by the product of the water/oil mobility ratio times the permeability contrast (Seright 2017).

For comparison, a three-injector pilot polymer flood in the Tambaredjo reservoir in Suriname explored injection of 45-125-cp HPAM solutions to displace 600-1700-cp oil (Moe Soe Let et al. 2012, Manichand et

al. 2013, Manichand and Seright 2014, Delamaide et al. 2016, Wang et al. 2017). The reservoir description indicated a 12:1 permeability contrast between two flooded zones—revealing potential for significant incremental oil recovery by injecting up to 200-cp polymer solutions (Moe Soe Let et al. 2012, Wang et al. 2017). Interestingly, an analysis of pilot performance by Delamaide et al. (2016) suggested that increasing viscosity beyond 45-cp did not result in any obvious increase in oil recovery. Additional analysis (Wang et al. 2017) indicated that a number of factors could have contributed to this finding including (1) a high compressibility of the formation, (2) the unconfined nature of the pilot project, (3) staged addition of two additional patterns to the original flood, (4) increases in injected polymer viscosity during the project, and (5) the condition of the wells (especially damage to production wells).

Conclusions

This paper examines oil displacement as a function of polymer solution viscosity during laboratory studies in support of a polymer flood in the Cactus Lake reservoir in Canada.

1. When displacing 1610-cp crude oil from field cores (at 27°C and 1 ft/d). oil recovery efficiency increased with polymer solution viscosity tip to 25 cp (7.3 s^{-1}). No significant benefit was noted from injecting polymer solutions more viscous than 25 cp.
2. No evidence was found that high-Mw HP AM solutions mobilized trapped residual oil in our application.
3. In nine field cores, relative permeability to water remained low—less than 0.03 for water saturations up to 0.42. Relative permeability to oil remained reasonably high (greater than 0.05) for most of this range. These observations help explain why only 25-cp polymer solutions were effective in recovering 1610-cp oil. The low relative permeability to water (<0.03) allowed 25-cp polymer to provide close to a favorable mobility ratio. At the same time, the relatively high relative permeability to oil (> 0.05) allowed oil behind the water front to continue flowing at a reasonable rate.
4. When plotted versus % of mobile oil recovered, seven polymer floods were consistent with fractional flow projections in that most of the mobile oil was efficiently recovered by polymers solutions with 25-cp viscosity (or greater).
5. During studies of saturation history in a field core (native state versus water-saturated first versus oil-saturated first), relative permeability to water showed similar shapes and trends for three cases with 1000-cp crude oil and one case with 1000-cp refined oil. However, the k_{rw} curve associated with the native-state core (perhaps the most oil wet?) was shifted most toward low water saturations, while the curve associated with the 1000-cp refine oil (probably the most water wet) was shifted most to high water saturations. Values for k_{rw} remained below 0.03 for much of the testing (up to water saturations of 0.63 for 1000-cp refined oil). Values for k_{ro} remained above 0.05 for a significant range of saturation.
6. During studies of the effects of oil viscosity (from 2.9 cp to 1000 cp) in a hydrophobic polyethylene core, relative permeability trends were consistent with previous literature—in that oil and water relative permeabilities were not sensitive to oil viscosity (for refined oils). However, they could depend on nature of the oil. At a given water saturation, relative permeability to water for 1000-cp crude oil was about ten times lower than for 1000-cp refined oil.
7. Our results were qualititatively consistent with the concepts developed by Doorwar and Mohanty (2017)—in that during waterflooding, apparent k_{rw} values were lower than expected and apparent *kro* values were higher than expected if no viscous fingering occurred. However, application of the fractional flow version of their concept under-predicted oil recovery when using 5-6-cp polymer solutions.

8. A viable explanation for the observed data for the 5-6-cp polymer solutions is that the resistance factors were 2-5 times higher than the viscosity suggests. Previous work demonstrated that this effect is a laboratory artifact that will not propagate deep into a reservoir.
9. Although 25-cp polymer solutions were effective in displacing oil during our core floods, the choice of polymer viscosity for a field application must consider reservoir heterogeneity and the enhanced risk of viscous fingering in a reservoir during unfavorable displacements.

Acknowledgements

Thanks to Tianguang Fan for measuring interfacial tensions and contact angles. The guidance of Alice Vickroy and Ray Sisson was deeply appreciated.

Nomenclature

D = core diameter, cm
k = permeability, darcys [^m^2]
k_{ro} = relative permeability to oil
k_{roo} = endpoint relative permeability to oil
k_{rw} = relative permeability to water
k_{rwo} = endpoint relative permeability to water
Mw = polymer molecular weight, g/mol
N_I = Doorwar/Mohanty viscous fingering stability parameter in Eq. 3, dimensionless
no = oil saturation exponent in Eq. 2
nw = water saturation exponent in Eq. 1
$OOIP$ = original oil in place, bbl [m^3]
PV = pore volumes of fluid injected
Δp = pressure difference, psi [Pa]
S_o = oil saturation
S_{or} = residual oil saturation
S_w = water saturation
S_{wi} = initial water saturation
v_w = flux, ft/d [m/d]
ϕ = porosity
λ = Doorwar/Mohanty viscous fingering parameter
μ_o = viscosity of oil, cp [mPa-s]
μ_w = viscosity of water, cp [mPa-s]
σ = interfacial tension mN/m

SI Metric Conversion Factors

cp × l.0*	E-03 = Pa·s
ft × 3.048*	E-01 = m
in. × 2.54*	E+00 = cm
md × 9.869 233	E-04 = μm^2
psi × 6.894 757	E+00 = kPa

References

Asghari, K. and Nakutnyy, P. 2008. Experimental Results of Polymer Flooding of Heavy Oil Reservoirs. Presented at the Canadian International Petroleum Conference, Calgary, Alberta, Canada, 17-19 June. PETSOC-2008-189. http://dx.doi.org/10.2118/2008-189.

Beliveau, D. 2009. Waterflooding Viscous Oil Reservoirs. *SPE Reservoir Eval. & Eng.* **12**(5): 689–701. http://dx.doi.org/10.2118/113132-PA.

Clarke, A., Howe, A. M., Mitchell, J., Staniland, J., & Hawkes, L. A. 2016. How Viscoelastic-Polymer Flooding Enhances Displacement Efficiency. *SPEJ* **21**(4): 675–687. http://dx.doi:10.2118/174654-PA.

Craig, F.F. 1971. *The Reservoir Engineering Aspects of Waterflooding*. Monograph Series, SPE, Richardson, Texas **3**: 4575.

Delamaide, E., Zaitoun, A., Renard, G., Tabary, R. 2014. Pelican Lake Field: First Successful Application of Polymer Flooding In a Heavy-Oil Reservoir. *SPE Reservoir Eval. & Eng.* **17**(3): 340–354. http://dx.doi.org/10.2118/165234-MS.

Delamaide, E., Let, K. M. S., Bhoendie, K., Paidin, W. R., & Jong-A-Pin, S. 2016. Interpretation of the Performance Results of a Polymer Flood Pilot in the Tambaredjo Oil Field, Suriname. SPE Annual Technical Conference and Exhibition held in Dubai, UAE, 26-28 September 2016. http://dx.doi:10.2118/181499-MS.

Doorwar, S., & Mohanty, K.K. 2017. Viscous-Fingering Fucntion for Unstable Immiscible Flows. *SPE Journal* **22**(1): 1931. http://dx.doi.org/10.2118/173290-PA.

Erincik, M. Z., Qi, P., Balhoff, M. T., & Pope, G. A. 2017. New Method to Reduce Residual Oil Saturation by Polymer Flooding. Presented at the SPE Annual Technical Conference and Exhibition. San Antonio, Texas. 9 October. http://dx.doi:10.2118/187230-MS.

Fabbri, C., Cottin, C., Jimenez, J., Nguyen, M., Hourcq, S., Bourgeois, M., & Hamon, G. 2014. Secondary and Tertiary Polymer Flooding in Extra-Heavy Oil: Reservoir Conditions Measurements - Performance Comparison. Presented at the International Petroleum Technology Conference. Doha, Qatar 20-22 January. http://dx.doi:10.2523/IPTC-17703-MS.

Geffen, T. M., Owens, W. W., Parrish, D. R., & Morse, R. A. 1951. Experimental Investigation of Factors Affecting Laboratory Relative Permeability Measurements. *Petroleum Transactions* **192**: 99–110. http://dx.doi:10.2118/951099-G.

Guo, H. (2017, November. How to Select Polymer Molecular Weight and Concentration to Avoid Blocking in Polymer Flooding? Presented at the SPE Symposium: Production Enhancement and Cost Optimisation, 7-8 November, Kuala Lumpur, Malaysia. http://dx.doi:10.2118/189255-MS

Johnson, E. F., Bossler, D. P., & Naumann, V. O. 1959. Calculation of Relative Permeability from Displacement Experiments. *Petroleum Transactions* **216**: 370–372. http://dx.doi:10.2118/951023-G.

Jones, S. C., & Roszelle, W. O. (1978, May 1). Graphical Techniques for Determining Relative Permeability from Displacement Experiments. *J. Pet. Tech:* 807–817. http://dx.doi:10.2118/6045-PA.

Koh, H., Lee, V. B., & Pope, G. A. (2017, August 1). Experimental Investigation of the Effect of Polymers on Residual Oil Saturation. *SPE Journal* **22**(1): 1–17. http://dx.doi:10.2118/179683-PA.

Kumar, M., Hoang, V., Satik, C., and Rojas, D. 2008. High-Mobility-Ratio-Waterflood Performance Prediction: Challenges and New Insights, *SPE Reservoir Eval. & Eng.* **11** (1): 186–196. http://dx.doi:10.2118/97671-PA.

Levitt, D., Jouenne, S., Bondino, I., Santanach-Carreras, E., & Bourrel, M. 2013. Polymer Flooding of Heavy Oil Under Adverse Mobility Conditions. Presented at the SPE Enhanced Oil Recovery Conference. Kuala Lumpur, Malaysia. 2-4 July. http://dx.doi:10.2118/165267-MS.

Liu J., Adegbesan, K., Bai., J. 2012. Suffield Area, Alberta, Canada—Caen Polymer Flood Pilot Project. Presented at the SPE Heavy Oil Conference, Calgary, Alberta, Canada, 12-14 June. SPE-157796-MS. http://dx.doi.org/10.2118/157796-MS.

Loubens, R. de, Vaillant, G., Regaieg, M., Yang, J., Moncorge, A., Fabbri, C., & Darche, G. (2017, February 20). Numerical Modeling of Unstable Water Floods and Tertiary Polymer Floods into Highly Viscous Oils. Presented at the SPE Reservoir Simulation Symposium. Mongomery, Texas. 20-22 February. http://dx.doi:10.2118/182638-MS.

Luo, H., Mohanty, K. K., & Delshad, M. (2017a, November 1). Modeling and Upscaling Unstable Water and Polymer Floods: Dynamic Characterization of the Effective Viscous Fingering. *SPE Reservoir Eval. & Eng.* **20** (4): 779–794. http://dx.doi:10.2118/179648-PA.

Luo, H., Delshad, M., Zhao, B., & Mohanty, K. K. (2017b, February 15). A Fractional Flow Theory for Unstable Immiscible Floods. Presented at the SPE Canada Heavy Oil Technical Conference. Calgary, Alberta, Canada. 15-16 February. http://dx.doi:10.2118/184996-MS.

Mai, A., and Kantzas, A. 2010. Mechanisms of Heavy Oil Recovery by Low Rate Waterflooding. *J. Canadian Petr. Tech.* **49**(1): 44–50. doi:10.2118/134247-PA.

Maini, B. 1998. Is it Futile to Measure Relative Permeability for Heavy Oil Reservoirs? *J. Canadian Petr. Tech.* **37**(4): 5662. http://dx.doi:10.2118/98-04-06

Manichand, R.N., Moe Soe Let, K.P., Gil, L. et al. 2013. Effective Propagation of HPAM Solutions through the Tambaredjo Reservoir during a Polymer Flood. *SPE Prod & Oper* **28**(4): 358–368. SPE-164121-PA. http://dx.doi.org/10.2118/164121-PA.

Manichand, R.N., and Seright, R.S. 2014. Field vs Laboratory Polymer Retention Values for a Polymer Flood in the Tambaredjo Field. *SPE Res Eval & Eng.* **17**(3): 314–325. SPE-169027-PA. http://dx.doi.org/10.2118/169027-PA.

Moe Soe Let, K.P., Manichand, R.N., and Seright, R.S. 2012. Polymer Flooding a ~500-cp Oil. Presented at the Eighteenth SPE Improved Oil Recovery Symposium, Tulsa, Oklahoma, USA, 14-18 April 2012. SPE-154567-MS. http://dx.doi.org/10.2118/154567-MS.

Odeh, A. S. 1959. Effect of Viscosity Ratio on Relative Permeability (includes associated paper 1496-G). *Petroleum Transactions* **216**: 346–351. doi:10.2118/951189-G.

Peters, E.J., and Flock, D.L. 1981. The Onset of Instability during Two-Phase Immiscible Displacement in Porous Media. *SPEJ*, April: 249–258. http://dx.doi:10.2118/8371-PA

Reichenbach-Klinke, R., Stavland, A., Strand, D., Langlotz, B., & Brodt, G. (2016, March 21). Can Associative Polymers Reduce the Residual Oil Saturation? Presented at the SPE EOR Converence at Oil and Gas West Asia. Muscat, Oman. 21-23 March. http://dx.doi:10.2118/179801-MS.

Richardson, J. G. (1957, May 1). *The Calculation of Waterflood Recovery from Steady-State Relative Permeability Data*. Society of Petroleum Engineers. http://dx.doi:10.2118/759-G.

Saboorian-Jooybari, H., Dejam, M., and Chen, Z. 2015. Half-Century of Heavy Oil Polymer Flooding from Laboratory Core Floods to Pilot Tests and Field Applications. Presented at the SPE Canada Heavy Oil Technical Conference, Calgary, Alberta, 9-11 June. SPE-174402-MS. http://dx.doi.org/10.2118/174402-MS.

Sandberg, C. R., Gournay, L. S., & Sippel, R. F. 1958. The Effect of Fluid-Flow Rate and Viscosity on Laboratory Determinations of Oil-Water Relative Permeabilities. *Petroleum Transactions* **213**: 36–43. http://dx.doi:10.2118/950709-G.

Seright, R. and Martin, F. 1993. Impact of Gelation pH, Rock Permeability, and Lithology on the Performance of a Monomer-Based Gel. *SPE Res Eng* **8**(1): 43–50. http://dx.doi.org/10.2118/20999-PA.

Seright, R., Prodanovic, M., and Lindquist, W. 2006. X-Ray Computed Microtomography Studies of Fluid Partitioning in Drainage and Imbibition Before and After Gel Placement: Disproportionate Permeability Reduction. *SPE Journal* **11**(2): 159–170. http://dx.doi.org/10.2118/89393-PA.

Seright, R.S. 2010. Potential for Polymer Flooding Viscous Oils. *SPE Reservoir Eval. & Eng.* **13**(3): 730–740. http://dx.doi:10.2118/129899-PA.

Seright, R.S., Fan, T., Wavrick, K., and Balaban, R.C. 2011. New Insights into Polymer Rheology in Porous Media. *SPE Journal* **16**(1): 35–42. http://dx.doi.org/10.2118/129200-PA.

Skauge, T., Vik, B. F., Ormehaug, P. A., Jatten, B. K., Kippe, V., Skjevrak, I., Standnes, D.C., Uleberg, K., Skauge, A. 2014. Polymer Flood at Adverse Mobility Ratio in 2D Flow by X-ray Visualization. Presented at the SPE EOR Conference at Oil and Gas West Asia, Muscat, Oman, 31 March-2 April. http://dx.doi:10.2118/169740-MS

Sorbie, K.S. and Seright, R.S. 1992. Gel Placement in Heterogeneous Systems with Crossflow. Presented at the SPE/DOE Symposium on Enhanced Oil Recovery, Tulsa, Oklahoma, USA, 22-24 April. http://dx.doi.org/10.2118/24192-MS.

Urbissinova, T. S., Trivedi, J., & Kuru, E. (2010, December 1). Effect of Elasticity during Viscoelastic Polymer Flooding: A Possible Mechanism of Increasing the Sweep Efficiency. *J. Canad. Petr. Tech.* **49**(12): 49–56. http://dx.doi:10.2118/133471-PA

Vermolen, E.C., Haasterecht, M.J.T., and Masalmeh, S.K. 2014. A Systematic Study of the Polymer Visco-Elastic Effect on Residual Oil Saturation by Core Flooding. Presented at the SPE EOR Conference at Oil and Gas West Asia, Muscat, Oman, 31 March-2 April. SPE-169681-MS. http://dx.doi.org/10.2118/169861-MS.

Vittoratos, E., and Kovseck, A.R. 2017. Doctrines and Realities in Reservoir Engineering. Presented at the SPE Wstern Regional Meeting. Bakersfield, California, 23-27 April. http://dx.doi.org/10.2118/185633-MS.

Wang, D., Huifen, X., Zhongchun, L. et al. 2000. Visco-Elastic Polymer Can Increase Microscale Displacement Efficiency in Cores. Presented at the 2000 SPE Annual Technical Conference and Exhibition, Dallas, Texas, USA, 1-4 October. SPE-63227-MS. http://dx.doi.org/10.2118/63227-MS.

Wang, D., Huifen, X., Zhongchun, L. et al. 2001a. Study of the Mechanism of Polymer Solution with Visco-Elastic Behavior Increasing Microscopic Oil Displacement Efficiency and the Forming of Steady "Oil Thread" Flow Channels. Presented at the 2001 SPE Asia Pacific Oil and Gas Conference and Exhibition, Jakarta, Indonesia, 17-19 April. SPE-68723-MS. http://dx.doi.org/10.2118/68723-MS.

Wang, D., Cheng, J., Xia, H. et al. 2001b. Viscous-Elastic Fluids Can Mobilize Oil Remaining after Water-Flood by Force Parallel to the Oil-Water Interface. Presented at the 2001 SPE Asia Pacific Improved Oil Recovery Conference, Kuala Lumpur, Malaysia, 8-9 October. SPE-72123-MS. http://dx.doi.org/10.2118/72123-MS.

Wang, D., Xia H., Yang, S. et al. 2010. The Influence of Visco-elasticity on Micro Forces and Displacement Efficiency in Pores, Cores and in the Field. Presented at the SPE EOR Conference at Oil and Gas West Asia, Muscat, Oman, 11-13 April. SPE-127453-MS. http://dx.doi.org/10.2118/127453-MS.

Wang, D., Wang, G., and Xia, H. 2011. Large Scale High Visco-Elastic Fluid Flooding in the Field Achieves High Recoveries. Presented at the SPE Enhanced Oil Recovery Conference, Kuala Lumpur, Malaysia, 19-21 July. SPE-144294-MS. http://dx.doi.org/10.2118/144294-MS.

Wang, D., Seright, R. S., Shao, Z., & Wang, J. 2008. Key Aspects of Project Design for Polymer Flooding at the Daqing Oilfield. *SPE Reservoir Eval. & Eng.* **11**(6): 1117–1124. http://dx.doi:10.2118/109682-PA

Wang, D., Seright, R.S., Moe Soe Let, K.P., et al. 2017. Compaction and Dilation Effects on Polymer Flood Performance. Presented at the SPE Europec featured at 79th EAGE Annual Conference & Exhibition held in Paris, France, 12-15 June 2017. SPE-185851-MS. http://dx.doi.org/10.2118/185851-MS.

Wang, J., Dong, M., & Asghari, K. (2006, January 1). *Effect of Oil Viscosity on Heavy Oil-Water Relative Permeability Curves*. Society of Petroleum Engineers. doi:10.2118/99763-MS.

Wang, J., and Dong, M. 2007. A Laboratory Study of Polymer Flooding for Improving Heavy Oil Recovery. Presented at the Canadian International Petroleum Conference, Calgary, Alberta, Canada, 12-14 June. PETSOC 2007-178. http://dx.doi.org/10.2118/2007-178.

Wassmuth, F.R., Green, K., Hodgins, L. et al. 2007. Polymer Flood Technology for Heavy Oil Recovery. Presented at the Canadian International Petroleum Conference, Calgary, Alberta, Canada, 12-14 June. PETSOC-2007-182. http://dx.doi.org/10.2118/2007-182.

Wassmuth, F.R., Arnold, W., Green, K. et al. 2009. Polymer Flood Application to Improve Heavy Oil Recovery at East Bodo. *J. Canad. Petr. Tech.* **48**(2): 1–7.

Willhite, G.P. 1986. Waterflooding. *SPE Textbook Series*, **3**: 21–110.